IEEE Access
Multidisciplinary | Rapid Review | Open Access Journal

Received 19 June 2023, accepted 26 July 2023, date of publication 28 July 2023, date of current version 3 August 2023.

Digital Object Identifier 10.1109/ACCESS.2023.3299871

RESEARCH ARTICLE

Memory Effects of High-Power Amplifiers in LSTM-Based Vehicular Channel Estimation

ANA FLÁVIA DOS REIS[1,2], (Student Member, IEEE), YAHIA MEDJAHDI[3], (Member, IEEE), BRUNO SENS CHANG[2], (Member, IEEE), GLAUBER BRANTE[2], (Senior Member, IEEE), AND C. FAOUZI BADER[4], (Senior Member, IEEE)

[1]Institut Supérieur d'Électronique de Paris (ISEP), 75006 Paris, France
[2]CPGEI, Federal University of Technology—Paraná (UTFPR), Curitiba 80230-901, Brazil
[3]Centre for Digital Systems, IMT Nord Europe, Institut Mines-Télécom, University of Lille, 59000 Lille, France
[4]Technology Innovation Institute, Abu Dhabi, United Arab Emirates

Corresponding author: Ana Flávia Dos Reis (anareis@alunos.utfpr.edu.br)

This work was supported in part by the Framework of the EcoTrain Project through the French Agency for Ecological Transition (ADEME) under Grant ADEME-"Digitalisation et Décarbonation du Transport Ferrovaire," in part by the National Council for Scientific and Technological Development (CNPq), under Grant 307226/2021-2 and Grant 402378/2021-0, and in part by the INESC P&D Brazil.

ABSTRACT The upcoming sixth generation (6G) of wireless communication systems is expected to enable a wide range of new applications in vehicular communication. However, the use of multicarrier-based modulation in vehicular communication introduces challenges due to the Doppler effects, which can induce nonlinear distortions at high-power amplifiers (HPAs) and significantly degrade channel estimation. In this paper, we investigate the performance of long short-term memory (LSTM)-based channel estimation considering the nonlinear HPA memory effects. Our results reveal the impact of these nonlinearities on the detection of transmitted signals, highlighting the importance of considering these often neglected effects when developing vehicular communication solutions for practical scenarios. We further present a low-complexity method for compensating for part of the NLD memory effects on the transmitter side, while handling the remaining distortions along with channel estimation. In addition, we emphasize the ability of certain estimators to handle these distortions at the receiver and present their advantages for tracking the vehicular channel.

INDEX TERMS Channel estimation, LSTM, HPA distortions, vehicular communication.

I. INTRODUCTION

Vehicular communication is one of the areas of greatest interest for the development of solutions within future 6G applications, where one of the challenges is to estimate the wireless channel with sufficient quality in order to ensure reliable communication. On this road, and along with the increase in the number of devices and the respective user requirements [1], vehicular communications will introduce challenges regarding the complexity of the solutions and their applicability to these highly variable and dynamic scenarios.

Vehicular communications employ multicarrier modulation techniques [2], among which orthogonal frequency division multiplexing (OFDM) is the most widely used scheme in modern standards, such as in the IEEE 802.11 and its variations [3]. However, the OFDM signal suffers from large peak-to-average power ratio (PAPR), *i.e.*, large amplitude variations, making this modulation very sensitive to nonlinear distortion (NLD) caused by high power amplifiers (HPA). These NLDs can impair the channel estimation and detection capability of the receivers, considerably degrading the system performance [4].

The literature presents two categories of HPA nonlinear models: memoryless and models with memory. In the first, both amplitude-to-amplitude modulation (AM/AM) and amplitude-to-phase modulation (AM/PM) conversion characteristics are functions of only the instantaneous amplitude of the signal applied to the HPA input, what can be considered as an approximation of the distortion effects. More realistic models also aim to capture the frequency-dependent

The associate editor coordinating the review of this manuscript and approving it for publication was Olutayo O. Oyerinde.

characteristics of the signal, in which the AM/AM and AM/PM functions of the HPA depend on the past input levels, such as in the models with memory effects [5]. There are different well-known representations of HPAs in wideband communications to approximate the nonlinear behavior with memory structures. For instance, Volterra models have been widely employed to model HPAs [6]. Nevertheless, besides allowing for a detailed analysis of the HPAs' behavior, the literature [6], [7] has recognized this model for its computational demands associated with higher-order kernels. This increasing complexity of these kernels can make the Volterra model less attractive from a theoretical perspective. Consequently, alternative models have been developed to provide simplifications and improve computational efficiency while still capturing essential aspects of HPA behavior [8]. In particular, we can refer to the Wiener and Hammerstein models, which consider a static nonlinear model used in series with a linear filter to model the memory effects [9].

Both Wiener and Hammerstein models are equivalent, with the Wiener model assuming a linear filter followed by a memoryless nonlinear block. In contrast, the Hammerstein model accounts for the memory effects by incorporating a linear filter after the nonlinearities. Examples employing Wiener HPA models can be found in [10] and [11], while Hammerstein HPA models are considered by [6] and [12], showing that it is possible to include this more realistic representation of the nonlinearities with dynamic memory effects in a cascade with the static (memoryless) NLD of the HPA. Usually, memoryless HPAs model well the narrowband behavior of the amplifiers. However, as a general trend, an increase in bandwidth is expected in the context of future communications, implying a stronger memory effect in the amplified signal. In addition, wideband HPAs usually provide higher power levels [13], while restricting amplifiers to the linear amplification range yields poor efficiency [14]. Despite that, the memory effects of the HPA is still a neglected factor in the design of channel estimator for vehicular communications in the literature.

Regarding channel estimation, due to its nature and requirements, mathematical estimators typically adopted by scenarios with low mobility might be less effective in tracking the vehicular channel estimation process. In this sense, deep learning-based solutions are gaining ground in vehicular communication, being capable of deploying flexible solutions that exploit the data generated by the network and make real-time decisions to, for example, track the channel [15]. In particular, long short-term memory (LSTM) structures are able to deal with sequential data, being capable of learning the channel correlation over time and efficiently predicting future channel realizations based on previous observations [16], [17]. The work in [16] proposes an LSTM-based estimator for tracking the vehicular channel, where a cascaded LSTM layer is employed after a shallow neural network (NN), which in its turn requires a coarse estimation performed by the data-pilot aided (DPA) method as the initial point. This method is able to learn the time and frequency characteristics of the channel and mitigate the noise in the estimation, improving performance when compared to other deep NN (DNN)-based receivers. Additionally, the authors in [17] apply a time averaging (TA) processing after the DPA method to alleviate the noise, which reduces the computational complexity of the NN compared to [16], while achieving similar performance. However, as shown in [4], all active subcarriers are required to perform the channel estimation in [16] and [17], requiring a large number of neurons to perform the operations on the LSTM units. Therefore, substantial computational complexity is a related problem for both estimators.

Our approach in [4] considers a DPA estimation prior to the LSTM layer, which enhances the overall error compensation due to the correlation introduced by the DPA. In addition, the proposed DPA-LSTM-NN method exploits the smooth variation of the vehicular channels with respect to the neighbor subcarriers in order to perform a sampling step, using fewer subcarriers at the input of the LSTM layer, considerably reducing complexity compared to [16] and [17]. In the present work, we take advantage of our previous analysis to extend the discussion regarding practical scenarios with NLDs. We highlight that, in contrast to frame-by-frame proposals [18], [19], our focus is on symbol-by-symbol (SBS) channel estimators, *i.e.*, in which the channel estimation is performed for each received symbol separately using only the previous and current received pilots, without increasing the latency of the application [15]. Thus, unlike [4], where only the memoryless HPA model was considered for the comparative analysis among the estimators, the effects of memory of the HPA model are now considered as an additional step to the analysis. Let us remark that the memoryless HPA model alone is an acceptable approximation for narrowband signals with nearly-constant envelope modulations. However, the distortion cancellation performance in scenarios with higher bandwidth or higher data rates is degraded if the memory effects of the HPA are neglected [6], [10], [11], [12]. Moreover, in contrast to digital linearization methods [20], where the nonlinear HPA is linearized from its inverse function modeled by a digital predistorter (DPD) before transmission, we present a method to compensate part of the memory NLD effects at the transmitter side using only a priori known HPA information, while handling the remaining distortions together with the channel estimation. The main contributions of this paper are summarized as follows:

- We analyze the impact of HPA memory effects on the performance of receivers proposed for vehicular channels. It is worth noting that in the literature on wireless channel estimators, a common practice has been to assume linear scenarios or employ memoryless HPA models. However, such approaches may not reflect reality, particularly when dealing with wideband signals or higher data rates. In these cases, the memory effects of HPAs become significant and can lead to severe performance degradation;
- We present a method to compensate part of the memory NLD effects on the transmitter side, while handling the

TABLE 1. List of acronyms adopted in this work.

Acronym	Meaning
6G	Sixth generation
AM/AM	Amplitude to Amplitude Modulation
AM/PM	Amplitude to Phase Modulation
BER	Bit Error Rate
CSI	Channel State Information
DNN	Deep Neural Network
DPA	Data-Pilot Aided
DPD	Digital Predistorter
FIR	Finite Impulse Response
FFT	Fast Fourier Transform
HPA	High Power Amplifier
IBO	Input Back-Off
ISI	Inter-Symbol-Interference
LoS	line-of-sight
LS	Least Square
LSTM	Long Short-Term Memory
NDL	Nonlinear distortion
NMSE	Normalized Mean Square Error
NN	Neural Network
OFDM	Orthogonal Frequency Division Multiplexing
PAPR	Peak-to-Average Power Ratio
R2V	Roadside-to-Vehicle
RMS	Root Mean Square
SBS	Symbol-by-symbol
SISO	Single-Input Single-Output
SNR	Signal-to-Noise Ratio
TA	Temporal Averaging
UC	Urban Canyon
V2V	Vehicle-to-Vehicle

TABLE 2. List of symbols adopted in this work.

Symbol	Meaning
K	Total number of subcarriers
K_{on}	Active subcarriers
K_{p}	Pilot subcarriers
$\mathcal{K}_{\text{on}}$	set of K_{on}
$\mathbf{y}_i[k]$	Received data for the k-th subcarrier in the i-th transmitted OFDM data symbol
$\mathbf{h}_i[k]$	Vectorized channel frequency response
$\mathbf{u}_i[k]$	Transmitted OFDM symbol affected by the HPA distortion
$\mathbf{x}_i[k]$	Transmitted OFDM symbol without effects from the HPA distortion
$\mathbf{n}_i[k]$	Gaussian noise
f_{D}	Doppler frequency
v	Speed of the vehicle
c	Speed of the light
f_{c}	Carrier frequency
$\tilde{\mathbf{u}}_{\text{mless}}(t)$	Output of the memoryless HPA
γ_0	Complex gain from the HPA
$\delta_i[k]$	Remaining NLD from the HPA
ϱ	Gain to ensure IBO
$\tau_{\mathbf{x}_i[k]}$	Mean power of the input signal
L	Number of OFDM symbols
ω	Coefficients of the FIR filter
$\mathbf{X}_{i,k}$	QAM data symbols for all k subcarriers within each i-th OFDM data symbol
$\mathbf{X}'_{i,k}$	Precoded QAM data symbols
$\mathbf{H}_{\text{FIR}\,k}$	Frequency response of the FIR filter for the k-th subcarrier
$\mathbf{x}(t)$	OFDM signal
$\mathbf{x}'(t)$	Precoded OFDM signal
α	Normalization factor for the effects of the FIR filter

remaining distortions along with the channel estimation. We highlight that this method does not add significant computational complexity to the transmission;
- We show that considering more realistic NLD models significantly affects receiver performance, and is an important aspect in developing estimators for future vehicular communication applications. Furthermore, the results highlight the importance of compensating the signal at the transmitter side when the memory effects of the HPA are considered.

The remainder of this paper is organized as follows. The system model is presented in Section II, while the main characteristics of the HPA NLD model, including the modeling of the nonlinear memory effects, are presented in Section III. Section IV presents a method considered to compensate for part of the memory effects from HPA. Results and discussions are presented in Section V and Section VI concludes the paper. For convenience, acronyms and symbols adopted in this work are summarized in Tables 1 and 2, respectively.

Notations: We use capital letters and lowercase letters in boldface to denote matrices and vectors, respectively. The notation $\exp(\cdot)$ denotes an exponential function, and $*$ denotes the convolution.

II. SYSTEM MODEL

Our system model considers the IEEE 802.11p standard [21], a subset of the Wi-Fi protocol based on OFDM waveform that uses 10 MHz frequency bandwidth and supports data transmission for roadside-to-vehicle (R2V) and vehicle-to-vehicle (V2V) communication. This standard specifies that every packet transmission consists of a preamble, a signal field that contains physical layer information, and a data field. The preamble has short and long training symbols, which the receiver uses for synchronization, and the long training symbols are split into two sequences to facilitate channel estimation. Additionally, a cyclic prefix is employed to combat the inter-symbol interference (ISI) caused by multi-path propagation.

Each OFDM symbol utilizes a total of $K = 64$ subcarriers in the data field, with $K_{\text{on}} = 52$ subcarriers being active and the remaining 12 serving as a guard band. Out of the K_{on} subcarriers, $K_{\text{p}} = 4$ are allocated as pilots, and the remaining 48 carry the actual data. For each active subcarrier $k \in \mathcal{K}_{\text{on}}$, with $\mathcal{K}_{\text{on}}$ being the set containing the K_{on} active subcarriers, the received OFDM symbols are expressed as

$$\mathbf{y}_i[k] = \mathbf{h}_i[k]\mathbf{u}_i[k] + \mathbf{n}_i[k], \tag{1}$$

where for all k subcarriers within the i-th OFDM symbol, $\mathbf{h}_i[k]$ denotes the time-variant frequency response of the subcarriers, $\mathbf{u}_i[k]$ is the k-th subcarrier in the i-th transmitted OFDM data symbol that is impacted by the HPA-induced distortions and $\mathbf{n}_i[k]$ represents the Gaussian noise.

The channel coefficients $\mathbf{h}_i[k]$ are modeled over a Rayleigh fading channel with Jakes' Doppler spectrum, with the Doppler frequency given by

$$f_{\text{D}} = \frac{v}{c} f_{\text{c}}, \tag{2}$$

where v is the speed of the vehicle, c is the speed of light and f_c is the carrier frequency.

III. HIGH POWER AMPLIFIER DISTORTION

We denote the output signal affected by the memory effects of the HPA as $\mathbf{u}(t)$, where t stands for the time domain index. Then, we employ the Hammerstein model [6], considering the memory effects in a cascade with the static nonlinearity of the HPA. Thus, we aim to explore HPA models that include memory, along with the mobility scenario, by taking into account accurate characterization of the effects of the HPA-induced nonlinearities in the analysis.

A. MEMORYLESS HPA

We first describe the memoryless HPA that will be used as a comparative basis for the case with the memory, denoting the input signal as $\mathbf{x}(t)$, which is assumed to be a zero mean complex Gaussian random process so that, following [5], we have the output given by

$$\tilde{\mathbf{u}}_{\text{mless}}(t) = \gamma_0 \mathbf{x}(t) + \tilde{\delta}(t), \tag{3}$$

where $\tilde{\delta}(t)$ is a NLD with zero mean and variance $\sigma_{\tilde{\delta}}{}^2$, that is uncorrelated with $\mathbf{x}(t)$, while γ_0 describes a complex gain. Then, according to the Bussgang theorem [22] γ_0 is compensated at the transmitter and we can write the output of the HPA as

$$\mathbf{u}_{\text{mless}}(t) = \mathbf{x}(t) + \delta(t), \tag{4}$$

where $\delta(t) = \tilde{\delta}(t)/\gamma_0$ is the remaining NLD of the HPA.

The memoryless polynomial model considered here follows [5], which exhibits AM/AM and AM/PM distortions by approximating its characterizations with a polynomial. Thus, for a given input signal $\mathbf{x}(t)$, the amplified output signal $\tilde{\mathbf{u}}_{\text{mless}}(t)$ can be expressed as

$$\begin{aligned}\tilde{\mathbf{u}}_{\text{mless}}(t) &= \phi_a\left(\rho(t)\right) \exp\left[j\left(\phi_p\left(\rho(t)\right) + \varphi(t)\right)\right] \\ &= \varsigma\left(\rho(t)\right) \exp\left(j\varphi(t)\right),\end{aligned} \tag{5}$$

in which $\rho(t)$ is the input signal modulus, $\varphi(t)$ is the input signal phase, $\phi_a\left(\rho(t)\right)$ and $\phi_p\left(\rho(t)\right)$ represent the AM/AM and AM/PM characteristics of the HPA respectively, while

$$\varsigma\left(\rho(t)\right) = \phi_a\left(\rho(t)\right) \exp\left[j\phi_p\left(\rho(t)\right)\right] \tag{6}$$

presents the complex soft envelope of the amplified output signal.

Moreover, the soft envelope of the amplified signal employed in our simulations is approximated by

$$\varsigma\left(\rho(t)\right) \approx \sum_{l=1}^{P} a_l \rho(t)^l, \tag{7}$$

where, according to the description of the polynomial model [5], a_l denotes the coefficients of the polynomial with order $P = 9$, obtained by the least square (LS) method.

To mitigate the impact of nonlinearities, the HPA is configured to operate at a specific Input Back-off (IBO), which is relative to the 1 dB compression point. This refers to the input power level where the amplifier's performance deviates by 1 dB from its linear behavior [23]. In this matter, before amplifying the signal by the HPA, it is scaled by the gain ϱ to ensure the desired IBO, given by

$$\varrho = \sqrt{\frac{\tau_{1\text{dB}}}{10^{\frac{\text{IBO}}{10}}\tau_{\mathbf{x}}}}, \tag{8}$$

where $\tau_{1\text{dB}}$ is the input power at 1 dB compression point and $\tau_{\mathbf{x}}$ is the mean power of the input signal.

B. MEMORY HPA

Future vehicular communication systems should require more complex HPA models for accurate analysis [12]. In these scenarios, the HPA memory effect can significantly impact the channel response, and ignoring it can lead to inaccurate channel estimates [13].

Figure 1 illustrates the transmitter side of the communication system modeled using a nonlinear HPA with memory, in which the Hammerstein model is constructed as a memoryless polynomial, described in Subsection III-A, in cascade with a finite impulse response (FIR) filter with F-taps. Following [6], we consider a FIR filter with $F = 3$ whose coefficients are given by $\boldsymbol{\omega} = [0.7692, 0.1538, 0.0769]$, obtained by measurements. It is noteworthy that ω can be modeled in practice either at the constructions of the HPA, or at a setup stage of the communication equipment.

Figure 2 shows the normalized magnitude of the frequency response of the HPA output as a function of the index of the subcarriers. Notice that the frequency response is not flat for the K_{on} subcarriers.[1]

IV. PROPOSED METHOD

A. COMPENSATION AT THE TRANSMITTER

In order to compensate for part of the HPA memory effects, a matched filter precoding is considered as a compensation block in Figure 1, ensuring a flat spectrum for all data subcarriers in the transmitted signal. The precoded QAM data symbols can be written as

$$\mathbf{X}'_{i,k} = \frac{\mathbf{X}_{i,k}}{\mathbf{H}_{\text{FIR}k}}, \tag{9}$$

where $\mathbf{H}_{\text{FIR}k}$ is the frequency response of the FIR filter for the k-th subcarrier, *i.e.*, it corresponds to the fast Fourier transform (FFT) of $\boldsymbol{\omega}$, and $\mathbf{X}_{i,k}$ presents the QAM data symbols for all k subcarriers within each i-th symbol. This strategy assigns a compensation step with low complexity to the transmitter. The result is shown in Figure 3, where we can observe a flat spectrum except for the 12 inactive subcarriers, alleviating signal degradation.

According to [5], since $\mathbf{x}(t)$ is an OFDM signal with a large number of subcarriers, it has zero mean normal distribution,

[1] Notice also that there are 12 inactive subcarriers, whose magnitudes are close to zero.

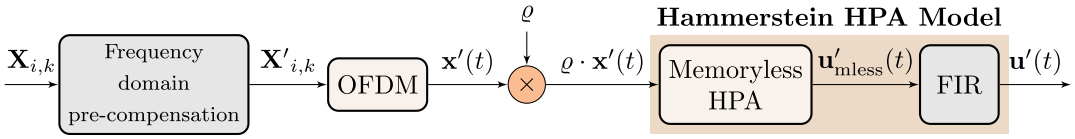

FIGURE 1. Transmission system model.

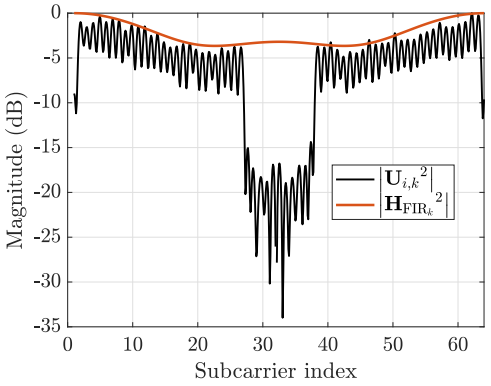

FIGURE 2. Frequency response of the HPA output without compensation.

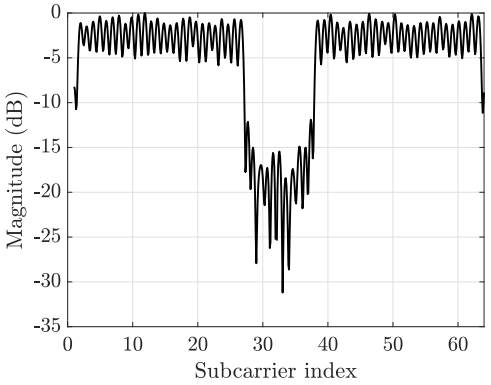

FIGURE 3. Frequency response of the HPA output compensated.

i.e., $\mathbf{x}(t) \sim \mathcal{N}(0, \vartheta)$, with ϑ being its variance. Thus, the frequency domain pre-compensation (as in Fig. 1) is equivalent to precoding $\mathbf{x}(t)$, so that

$$\mathbf{x}'(t) = \mathbf{g}(t) * \mathbf{x}(t) \tag{10}$$

where $\mathbf{g}(t)$ is obtained as the inverse FFT of $\frac{1}{\mathbf{H}_{\text{FIR}\,k}}$. As proven by [24], since $\mathbf{x}'(t)$ is a linear combination of uncorrelated normally distributed random variables, it also yields a normally distributed random variable, such that $\mathbf{x}'(t) \sim \mathcal{N}(0, \vartheta')$, where ϑ' depends on coefficients of $\frac{1}{\mathbf{H}_{\text{FIR}\,k}}$. Let us remark that this is crucial in order to apply the Bussgang theorem in (4) and validate the polynomial approximation in (7) while compensating the signal. In other words, even by introducing the compensation stage and the FIR filter of the Hammerstein model, the relations assumed in (4)-(7) are still valid.

Finally, the signal $\mathbf{x}(t)$ is normalized using a root mean square (RMS) normalization, while the output signal $\mathbf{u}(t)$ is normalized according to the effects of the FIR filter, being divided by the factor

$$\alpha = \sqrt{\sum_{f=1}^{F} \omega_f^2}. \tag{11}$$

B. DPA-LSTM-NN AT THE RECEIVER

At the receiver, we employ the DPA-LSTM-NN method proposed in [4], whose three main structures are fundamental to achieving good performance face to the HPA NLDs. In addition, as presented in its block diagram in Figure 4, the DPA-LSTM-NN considers a subcarrier sampling at the input of the LSTM, so that it interpolates the subcarriers' information to reduce the complexity of the solution. The key feature of the method compared to the preamble-based LS estimation used in [16] and [17] is first to consider a more reliable initial estimate, by means of the DPA estimation. The DPA is able to learn the time and frequency characteristics of the channel and reconstruct the estimation as close as possible to the ideal channel response. Then, the LSTM structure is designed to deal with sequential data, being capable of learning the channel correlation over time and efficiently predicting future channel realizations based on previous observations. This is crucial to handle the memory effects of the HPA. Furthermore, a NN is employed as an additional noise compensation step.

As a consequence, the combination of the compensation step at the transmitter described in Subsection IV-A and the DPA-LSTM-NN scheme at the receiver results in a communication system robust to the effects of memory of the HPA. Finally, we highlight that the work in [4] provides a detailed comparison between the DPA-LSTM-NN scheme and other estimators in the literature, both in terms of performance and complexity. As a result, the DPA-LSTM-NN scheme also exhibits lower complexity than [16] and [17].

V. SIMULATION RESULTS

We take advantage of the performance gain of the LSTM-based over traditional DNN-based receivers in SBS estimation. Thus, here we compare the LSTM-NN-DPA [16], LSTM-DPA-TA [17], and DPA-LSTM-NN [4] estimators in scenarios with HPA models with memory effects. The LSTM-NN-DPA scheme has been proposed in [16] and employs a cascaded LSTM layer after a NN in order to,

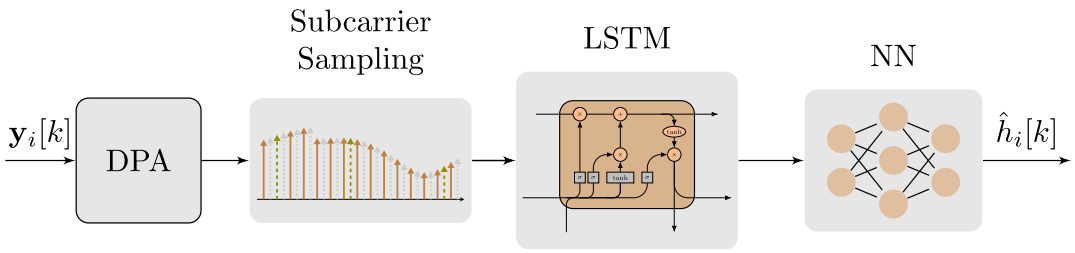

FIGURE 4. Block diagram of the DPA-LSTM-NN estimator [4].

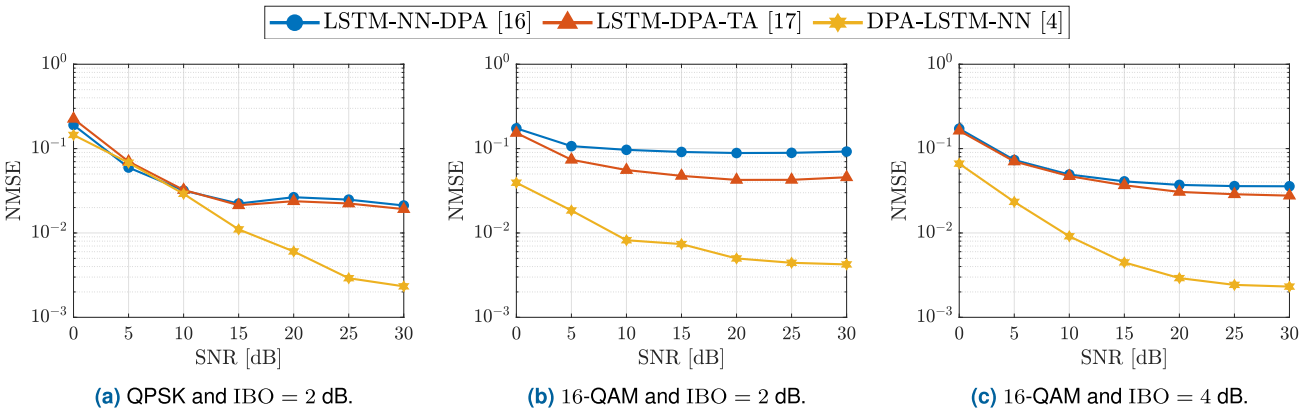

(a) QPSK and IBO = 2 dB. (b) 16-QAM and IBO = 2 dB. (c) 16-QAM and IBO = 4 dB.

FIGURE 5. NMSE performance in the scenario with NLD memory effects.

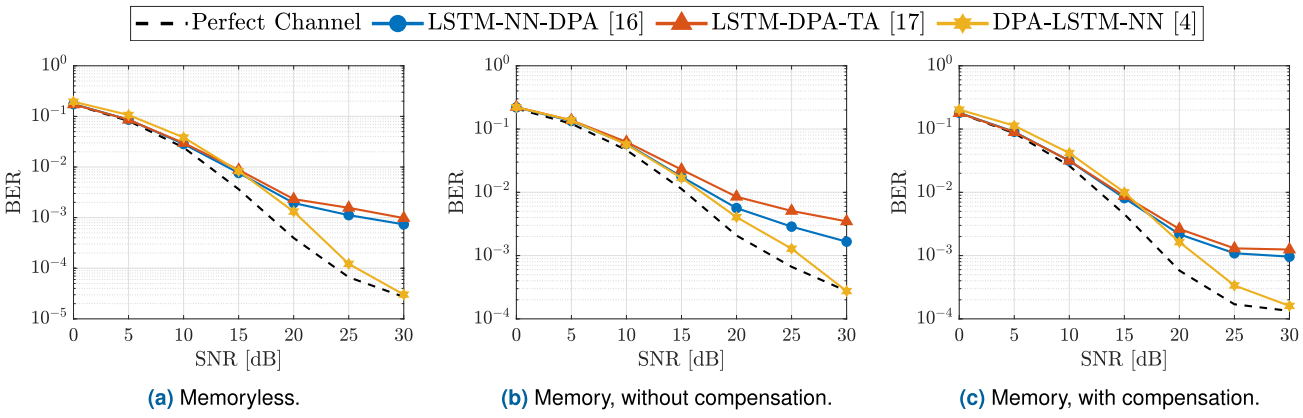

(a) Memoryless. (b) Memory, without compensation. (c) Memory, with compensation.

FIGURE 6. BER performance using QPSK modulation, v = 50 km/h and IBO = 2 dB.

TABLE 3. Real-valued operations for the considered channel estimators.

Channel Estimator	Multiplications/Divisions	Summations/Subtractions
LSTM-NN-DPA [16]	$12\,K_{\text{on}}{}^2 + 82\,K_{\text{on}} + 8\,K_{\text{on}}\,K_{\text{p}}$	$90K_{\text{on}} + 8\,K_{\text{p}} - 8$
LSTM-DPA-TA [17]	$12\,K_{\text{on}}{}^2 + 24\,K_{\text{on}}$	$32K_{\text{on}} - 8$
DPA-LSTM-NN [4]	$3\,K_{\text{on}}{}^2 + 3\,K_{\text{p}}{}^2 + 6\,K_{\text{on}}\,K_{\text{p}} + 161/2\,K_{\text{on}} + 3/2\,K_{\text{p}}$	$159/2\,K_{\text{on}} + 21/2\,K_{\text{p}} - 8$

considering a coarse initial estimation, reconstruct the channel as close as possible to the ideal channel response. This method is able to learn the time and frequency characteristics of the channel, tracking its variation and compensating the noise in the estimation, while presenting significant performance improvement when compared to DNN-based receivers. However, this is at the cost of higher computational complexity. By its turn, the LSTM-DPA-TA [17] applies time averaging (TA) processing after the DPA procedure, considering it as a noise alleviation technique, and reducing part of the computational complexity related to the NN in [16], while achieving similar performance. Nevertheless, as presented in [4], both receivers require all active subcarriers to perform the channel estimation. This leads to a large number of neurons to perform the operations on the LSTM units, presenting huge computational complexity. In the present work, we aim to compare these estimators and analyze the impact of the NLD induced by the HPAs and the gains when compensating the input signal for different modulations and levels of nonlinearities. To support

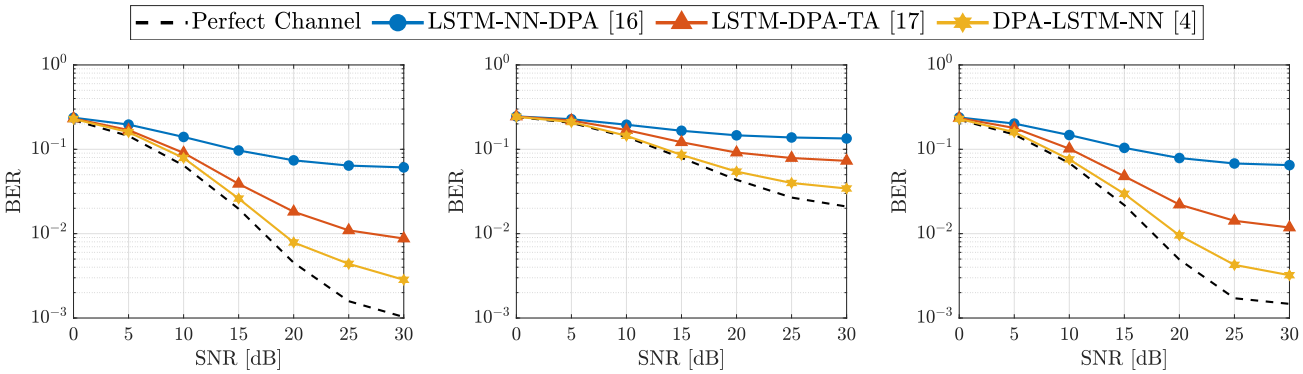

(a) Memoryless. (b) Memory, without compensation. (c) Memory, with compensation.

FIGURE 7. BER performance using 16-QAM modulation, $v = 50$ km/h and IBO = 2 dB.

reproducibility, the codes used for the simulated results can be downloaded at [25].

We plot the estimators' normalized mean squared error (NMSE) and bit error rate (BER) performance considering a transmitted OFDM frame size of $L = 50$ symbols. For all schemes, we consider a convolutional encoder with code rate 1/2 at the transmitter and a Viterbi decoder at the receiver, as defined by the IEEE 802.11p standard [21]. Furthermore, the roadside-to-vehicle Urban Canyon (R2V-UC) [26] model is considered to deploy the communication channel between a transmitting antenna mounted on a roadside and a receiver vehicle approaching, modeling a single-input single-output (SISO) transmission with line-of-sight (LoS). The analysis is performed with a speed of $v = 50$ km/h, but it should be noted that the results are qualitatively similar at other speeds.

Figure 5 presents the NMSE performance for the wireless channel affected by the impairments related to the memory HPA. Let us highlight that this metric is calculated as the error between the channel estimated for each receiver and the perfect channel, *i.e.* the channel where channel state information (CSI) is known. The estimators' performance is almost identical at a low signal-to-noise ratio (SNR) in the scenario with QPSK modulation and IBO = 2 dB, presented in Figure 5(a). However, when the SNR is greater than 10 dB, the DPA-LSTM-NN [4] outperforms the other methods since the DPA provides more reliable information to the LSTM layer when compared to the LS used by [16] and [17]. Moreover, in the scenarios with 16-QAM modulation presented in Figures 5(b) and 5(c), we observe an advantage of the DPA-LSTM-NN estimator, that outperforms the other solutions regardless of the SNR. This highlights the gain of this estimator for the case of higher modulation orders, while the other receivers suffer from a huge estimation error.

Figure 6 presents the BER performance of the LSTM-based estimation schemes using QPSK modulation and IBO = 2 dB. Besides focusing on the memory HPA, the performance with a memoryless HPA model is also shown for comparison purposes. In addition, the effects with and without the compensation done by (9) are also put side-by-side. The comparison of Figures 6(a) and 6(b) reveals a loss of at least 6 dB to achieve a BER below 10^{-3}. Despite this, the HPA memory compensation is shown in Figure 6(c), where the loss is reduced to less than 1 dB to achieve the same error rate, achieving a performance closer to the memory scenario for all the estimators considered. Still, for all cases considered and in agreement with the NMSE result, the DPA-LSTM-NN estimator proposed in [4] outperforms the other solutions in high SNR scenarios.

The effects of HPA modeling are shown in Figure 7, where memory effects severely degrade system performance with IBO = 2 dB and higher modulation order (16-QAM). Comparing Figures 7(a) and (b), a significant BER increase is observed due to the memory effects. By its turn, Figure 7(c) shows effective compensation using the proposed method. We remark that the compensation in (9) is practical since the FIR coefficients $\boldsymbol{\omega}$ need only to be estimated based on numerical measurements given the employed HPA, presenting a method where no high computational complexity is required on the transmitter side. In particular, K_{on} real-valued operations in terms of multiplications/divisions and sums/subtractions are required at the pre-compensation step, representing 1.65% of the global complexity to estimate the channel from a received OFDM symbol. Therefore, based on [4], the total number of operations necessary for each one of the methods is presented in Table 3, with the DPA-LSTM-NN presenting a complexity reduction of 49.74% when compared to the LSTM-NN-TA and of 58.76% when compared to the LSTM-NN-DPA. Additionally, the DPA-LSTM-NN method outperforms other estimators in the presence of HPA memory effects, maintaining similar performance as shown in Figures 7(a) and (c). Furthermore, regardless of whether the compensation is performed in the transmitter, DPA-LSTM-NN shows an advantage over other solutions in scenarios with HPA memory effects. This indicates that the LS estimation used as the input of the LSTM layers in [16] and [17] is highly degraded by the HPA NLD effects.

Finally, Figure 8 presents the BER with 16-QAM modulation and IBO = 4 dB, *i.e.*, smoother nonlinear effects. Again, the DPA-LSTM-NN performs better in minimizing the error between the perfect channel and its channel estimates, being

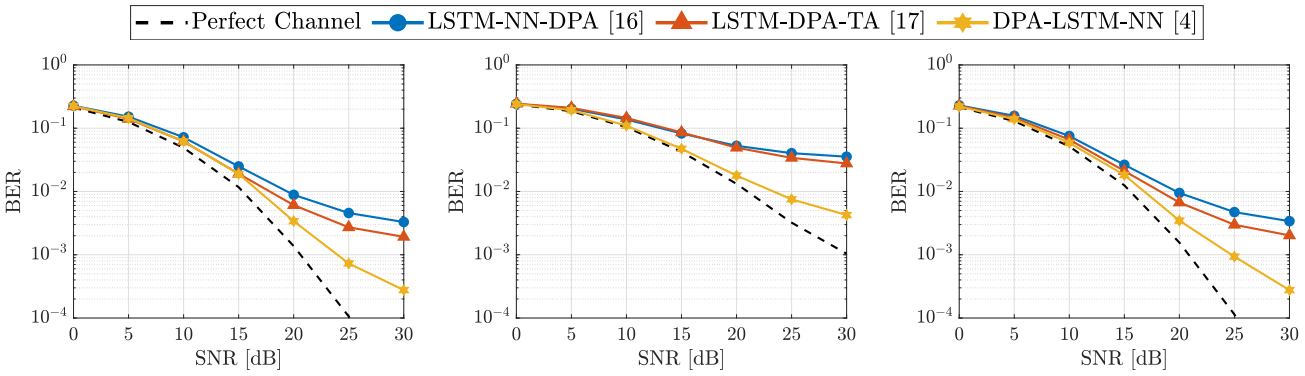

(a) Memoryless. (b) Memory, without compensation. (c) Memory, with compensation.

FIGURE 8. BER performance for 16-QAM modulation, $v = 50$ km/h and IBO $= 4$ dB.

a better choice for tracking the channel in the presence of NLD with memory. Figure 8(c) shows that the compensation done at the transmitter side significantly improves the performance for all estimators. Here, we underline the importance of this compensation step, showing that from a sufficiently robust estimator (such as the one presented in [4]), a compensation by means of (9) is sufficient to improve the communication performance. This effect becomes evident by comparing Figure 8(b) and Figure 8(c), since a BER below 10^{-3} can only be obtained when the compensation stage is considered at the transmitter. In addition, when comparing the DPA-LSTM-NN estimator with [16] and [17], we can observe that DPA-LSTM-NN is the sole capable of reaching a BER in the order of 10^{-3}, while both LSTM-NN-DPA and LSTM-DPA-TA estimators present an error floor at high SNR.

VI. CONCLUSION

This work analyzes the impact of HPA nonlinearities on the performance of channel estimation schemes used in vehicular communication, according to different proposed models. Our results show that the use of more realistic NLD models generates a relevant impact on the receivers' performances, being an important aspect in the development of estimators for future vehicular communication applications. Furthermore, the results highlight the importance of compensating the signal at the transmitter side when the memory effects of the HPA are considered, with this stage being essential to achieving a BER below 10^{-3} in the scenario with 16-QAM modulation and IBO $=$ 4 dB, for example. Also importantly, the DPA-LSTM-NN estimator presents to be robust face to the memory effects of the HPA, as it outperforms other estimators in terms of NMSE performance and has an almost negligible error rate performance gap when comparing scenarios with memoryless HPAs and memory HPAs with compensation. In future work, we intend to investigate different modulation techniques that are suitable for vehicular communication scenarios, evaluating their performance in mitigating the effects of NLD induced by HPAs.

REFERENCES

[1] W. Tong and P. Zhu, *6G: The Next Horizon: From Connected People and Things to Connected Intelligence*. Cambridge, U.K.: Cambridge Univ. Press, 2021.

[2] N. D. Lahbib, M. Cherif, M. Hizem, and R. Bouallegue, "BER analysis and CS-based channel estimation and HPA nonlinearities compensation technique for massive MIMO system," *IEEE Access*, vol. 10, pp. 27899–27911, 2022.

[3] B. Farhang-Boroujeny and H. Moradi, "OFDM inspired waveforms for 5G," *IEEE Commun. Surveys Tuts.*, vol. 18, no. 4, pp. 2474–2492, 4th Quart., 2016.

[4] A. F. Dos Reis, Y. Medjahdi, B. S. Chang, J. Sublime, G. Brante, and C. F. Bader, "Low complexity LSTM-NN-based receiver for vehicular communications in the presence of high-power amplifier distortions," *IEEE Access*, vol. 10, pp. 121985–122000, 2022.

[5] H. Shaiek, R. Zayani, Y. Medjahdi, and D. Roviras, "Analytical analysis of SER for beyond 5G post-OFDM waveforms in presence of high power amplifiers," *IEEE Access*, vol. 7, pp. 29441–29452, 2019.

[6] T. Wang and J. Ilow, "Compensation of nonlinear distortions with memory effects in OFDM transmitters," in *Proc. IEEE Global Telecommun. Conf.*, Nov. 2004, pp. 2398–2403.

[7] D. R. Morgan, Z. Ma, J. Kim, M. G. Zierdt, and J. Pastalan, "A generalized memory polynomial model for digital predistortion of RF power amplifiers," *IEEE Trans. Signal Process.*, vol. 54, no. 10, pp. 3852–3860, Oct. 2006.

[8] P. L. Gilabert, G. Montoro, and E. Bertran, "On the Wiener and Hammerstein models for power amplifier predistortion," in *Proc. Asia–Pacific Microw. Conf. Proc.*, 2005, p. 4.

[9] Y. Zhang, B. Li, N. Wu, Y. Ma, W. Yuan, and L. Hanzo, "Message passing-aided joint data detection and estimation of nonlinear satellite channels," *IEEE Trans. Veh. Technol.*, vol. 72, no. 2, pp. 1763–1774, Feb. 2023.

[10] S. Chen, "An efficient predistorter design for compensating nonlinear memory high power amplifiers," *IEEE Trans. Broadcast.*, vol. 57, no. 4, pp. 856–865, Dec. 2011.

[11] Y. Moegiharto, A. M. K. Bebyrahma, and I. Anisah, "BER performance of joint PTS PAPR reduction technique and Wiener HPA predistortion in OFDM system," in *Proc. Int. Electron. Symp. (IES)*, Sep. 2019, pp. 480–484.

[12] R. Zayani, R. Bouallegue, and D. Roviras, "Adaptive predistortions based on neural networks associated with Levenberg–Marquardt algorithm for satellite down links," *EURASIP J. Wireless Commun. Netw.*, vol. 2008, no. 1, pp. 1–15, Dec. 2008.

[13] A. R. Belabad, S. A. Motamedi, and S. Sharifian, "An adaptive digital predistortion for compensating nonlinear distortions in RF power amplifier with memory effects," *Integration*, vol. 57, pp. 184–191, Mar. 2017.

[14] D. Chowdhury, C. D. Hull, O. B. Degani, Y. Wang, and A. M. Niknejad, "A fully integrated dual-mode highly linear 2.4 GHz CMOS power amplifier for 4G WiMax applications," *IEEE J. Solid-State Circuits*, vol. 44, no. 12, pp. 3393–3402, Dec. 2009.

[15] A. K. Gizzini and M. Chafii, "A survey on deep learning based channel estimation in doubly dispersive environments," *IEEE Access*, vol. 10, pp. 70595–70619, 2022.

[16] J. Pan, H. Shan, R. Li, Y. Wu, W. Wu, and T. Q. S. Quek, "Channel estimation based on deep learning in vehicle-to-everything environments," *IEEE Commun. Lett.*, vol. 25, no. 6, pp. 1891–1895, Jun. 2021.
[17] A. K. Gizzini, M. Chafii, S. Ehsanfar, and R. M. Shubair, "Temporal averaging LSTM-based channel estimation scheme for IEEE 802.11p standard," in *Proc. IEEE Global Commun. Conf. (GLOBECOM)*, Dec. 2021, pp. 01–07.
[18] M. Soltani, V. Pourahmadi, A. Mirzaei, and H. Sheikhzadeh, "Deep learning-based channel estimation," *IEEE Commun. Lett.*, vol. 23, no. 4, pp. 652–655, Apr. 2019.
[19] A. K. Gizzini, M. Chafii, A. Nimr, R. M. Shubair, and G. Fettweis, "CNN aided weighted interpolation for channel estimation in vehicular communications," *IEEE Trans. Veh. Technol.*, vol. 70, no. 12, pp. 12796–12811, Dec. 2021.
[20] M. F. Haider, F. You, S. He, T. Rahkonen, and J. P. Aikio, "Predistortion-based linearization for 5G and beyond millimeter-wave transceiver systems: A comprehensive survey," *IEEE Commun. Surveys Tuts.*, vol. 24, no. 4, pp. 2029–2072, 4th Quart., 2022.
[21] *IEEE Guide for Wireless Access in Vehicular Environments (WAVE)—Architecture*, IEEE Standard 1609.0-2013, 2014, pp. 1–78.
[22] J. J. Bussgang, "Crosscorrelation functions of amplitude-distorted Gaussian signals," Res. Lab. Electron., MIT, Cambridge, MA, USA, Tech. Rep., 216, 1952.
[23] P. Colantonio, F. Giannini, and E. Limiti, *High Efficiency RF and Microwave Solid State Power Amplifiers*. Hoboken, NJ, USA: Wiley, 2009.
[24] B. Eisenberg and R. Sullivan, "Why is the sum of independent normal random variables normal?" *Math. Mag.*, vol. 81, no. 5, pp. 362–366, Dec. 2008.
[25] A. F. Dos Reis. *LSTM-Based Estimation With Memory HPA*. Accessed: May 10, 2023. [Online]. Available: https://github.com/anafreis/LSTM-Based-estimation-MemoryHPA
[26] G. Acosta-Marum and M. A. Ingram, "Six time- and frequency—Selective empirical channel models for vehicular wireless LANs," *IEEE Veh. Technol. Mag.*, vol. 2, no. 4, pp. 4–11, Dec. 2007.

ANA FLÁVIA DOS REIS (Student Member, IEEE) was born in Curitiba, Brazil, in 1996. She received the B.Sc. degree in automation engineering and the M.Sc. degree in telecommunications and networks from the Federal University of Technology—Paraná (UTFPR), Curitiba, in 2017 and 2020, respectively. She is currently pursuing the joint Ph.D. degree in a cotutelle between the Institut Supérieur dÉlectronique de Paris (ISEP), Paris, France, and UTFPR. Her research interests include wireless communications, vehicular communications, energy efficiency, and machine learning.

YAHIA MEDJAHDI (Member, IEEE) received the Engineering degree from the National Polytechnic School, Algiers, the M.Sc. degree in signal processing for communications from Institute Galilée, University of Paris XIII, in 2008, and the Ph.D. degree from Conservatoire National des Arts et Métiers (CNAM), in July 2012. He is currently an Associate Professor with the Centre for Digital Systems, IMT Nord Europe, Lille. Prior to that, he was an Associate Professor with Institut Supérieur déElectronique de Paris (ISEP), a Researcher with the CEDRIC Laboratory, CNAM, an Assistant Professor with Khemis-Miliana University, Algeria, and a Postdoctoral Researcher with the ICTEAM Laboratory, Université Catholique de Louvain (UCL), Belgium. He has been involved in several ICT-European and French projects (PHYDYAS, EMPHATIC, and WONG5) dealing with waveform design for 5G and PMR systems. His research interests include waveform design for beyond-5G, channel estimation, PAPR reduction, and non-linearity of power amplifiers.

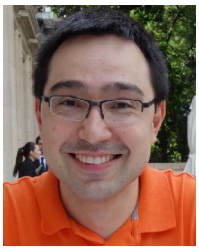

BRUNO SENS CHANG (Member, IEEE) was born in Curitiba, Brazil, in 1984. He received the B.Sc. degree in telecommunications engineering from the Regional University of Blumenau (FURB), Brazil, in 2006, the M.Sc. degree in electrical engineering from the Federal University of Santa Catarina (UFSC), Florianópolis, Brazil, in 2008, and the joint D.Sc. degree in electrical engineering from UFSC, and the Conservatoire National des Arts et Métiers (CNAM), Paris, France, in 2012. He was an invited Professor with CNAM, in 2018. He is currently an Associate Professor with the Federal University of Technology—Paraná (UTFPR), Curitiba. His current research interests include signal processing, channel estimation, interference reduction, and waveform design for next generation communication systems.

GLAUBER BRANTE (Senior Member, IEEE) received the Ph.D. degree in electrical engineering from the Federal University of Technology–Paraná (UTFPR), Curitiba, Brazil, in 2013. In 2012, he was a Visiting Researcher with the Institute of Information and Communication Technologies, Electronics, and Applied Mathematics, Catholic University of Louvain, Belgium. He is currently an Assistant Professor with UTFPR. His research interests include wireless communications, machine-type communications, energy efficiency, and energy harvesting. He was a recipient of the Best Ph.D. Thesis Award in electrical engineering in Brazil, in 2014. He was a co-recipient of the 2016 Research Award from the Cuban Academy of Sciences. He was the Co-Editor-in-Chief of the *Journal of Communication and Information Systems*, from 2018 to 2020. Since 2018, he has been an Associate Editor of the IEEE Communications Letters, since 2019, he has been serving as an Associate Editor for the IEEE Open Journal of the Communications Society, and since 2022, he has been serving as an Associate Editor for the IEEE Wireless Communications Letters.

C. FAOUZI BADER (Senior Member, IEEE) received the Ph.D. degree (Hons.) in telecommunications from Universidad Politécnica de Madrid (UPM), Madrid, Spain, in 2001. He joined the Centre Technologic de Telecomunicacions de Catalunya (CTTC), Barcelona, Spain, as a Research Associate, in 2002, and from 2006 to 2013, he was a Senior Research Associate. From June 2013 to December 2013, he was an Associate Professor with CentraleSupélec, France. Since 2017, he has been an Honorary Adjunct Professor with the University of Technology Sydney, Australia, and from 2018 to 2019, he was the Head of the Signals and Communications Department, Institute of Electronics and Digital Technologies (IETR), Rennes, France. From 2020 to 2021, he was the Director of Research with Institut Supérieur déElectronique de Paris (ISEP), France. Since December 2021, he has been the Director Telecom of the DSRC Centre, Technology Innovation Institute (TII), Abu Dhabi, United Arab Emirates. His research interests include IMT-advanced systems, such as 5G networks and systems, cognitive radio communication environment, and THz wireless communications (6G). He has been involved in several European projects from the fifth to seventh EC research frameworks (eight EU funded projects and ten national projects). He has been the main Coordinator of the BRAVE ANR French Project, CentraleSupélec, where the main goal was the achievement of efficient waveform for THz/Terabits wireless communication devices. He has published over 45 journals, 136 papers in peer-reviewed international conferences, more than 13 book chapters, and four edited books. He served as a Technical Program Committee Member of major IEEE ComSoc and VTS Conferences (ICC, PIMRC, VTC spring/fall, WCNC, ISWCS, GLOBECOM, and ICT).